Palladium Complexes with 3-Alkyl-Substituted-1,10-Phenanthrolines: Effect of the Remote Alkyl Substituent on the CO/Olefin Copolymerization Reactions

ARTICLE *in* ORGANOMETALLICS · NOVEMBER 2004

Impact Factor: 4.13 · DOI: 10.1021/om0493412

10 AUTHORS, INCLUDING:

Barbara Milani
Università degli Studi di Trieste
68 PUBLICATIONS **1,536** CITATIONS
SEE PROFILE

Ennio Zangrando
Università degli Studi di Trieste
75 PUBLICATIONS **1,286** CITATIONS
SEE PROFILE

Mauro Stener
Università degli Studi di Trieste
161 PUBLICATIONS **2,628** CITATIONS
SEE PROFILE

Sara Furlan
Bracco Imaging, Ivrea, Italy
33 PUBLICATIONS **398** CITATIONS
SEE PROFILE

Palladium Complexes with 3-Alkyl-Substituted-1,10-Phenanthrolines: Effect of the Remote Alkyl Substituent on the CO/Olefin Copolymerization Reactions

Alessandro Scarel, Barbara Milani,* Ennio Zangrando, Mauro Stener, Sara Furlan, Giovanna Fronzoni, and Giovanni Mestroni

Dipartimento di Scienze Chimiche, Università di Trieste, Via Licio Giorgieri 1, 34127 Trieste, Italy

Serafino Gladiali

Dipartimento di Chimica, Università di Sassari, Via Vienna 2, 07100 Sassari, Italy

Carla Carfagna and Luca Mosca

Istituto di Scienze Chimiche, Università di Urbino, Piazza Rinascimento 6, 61029 Urbino, Italy

Received August 23, 2004

The coordination chemistry of a series of 3-alkyl-substituted-1,10-phenanthrolines (3-R-phen) to palladium as well as the catalytic behavior of the corresponding bischelated derivatives, $[Pd(3\text{-R-phen})_2][PF_6]_2$, in the CO/vinyl arenes copolymerization reaction has been investigated in detail. The alkyl substituents differ in length and steric hindrance. The crystal structure characterization reveals that the two molecules of 3-R-phen are bound to palladium in a *syn* arrangement with the alkyl groups on the same side of the square planar geometry. In solution a dynamic process involving the equilibrium between *syn* and *anti* isomers is evidenced by NMR spectroscopic analysis. This is in agreement with the results of DFT calculations, which indicate similar stabilities for the two isomers. The severe distortions from the ideal square planar coordination geometry observed in the solid state are rationalized, through the DFT analysis, in terms of the HOMO orbitals responsible for the Pd−N bonds. The $[Pd(3\text{-R-phen})_2][PF_6]_2$ complexes efficiently promote the CO/styrene and CO/*p*-Me-styrene copolymerizations to the corresponding syndiotactic polyketones. Yields and molecular weights show an increasing trend on increasing the steric demand of the R substituent, and the values recorded are the best ones ever reported for copolymerization reactions of this kind in the absence of the oxidant. From the TON numbers this result seems related to an increase of the olefin insertion rate, which proceeds faster when 3-R-phen are used as ligands. A change of the physical nature of the active species, from homogeneous to heterogeneous, occurs during the polymerization process, and the time at which this variation takes place depends on the nature of the olefin. The positive effect of the alkyl substitution is less evident in the CO/ethylene copolymerization.

Introduction

During the last 10 years in homogeneous catalysis there has been an increasing use of transition metal complexes with heterocyclic sp^2 nitrogen-donor ligands.[1] In particular, much attention has been addressed to chiral bidentate chelating ligands with 2,2′-bipyridine or 1,10-phenanthroline framework.[2] Moreover, much effort has been devoted to the development of new polymeric materials having controlled architectures.[3] Among the new polymers studied in the past decade, the polyketones originating from carbon monoxide/olefin copolymerization have attracted much attention from both the academic and industrial scientific world.[4]

This copolymerization reaction is homogeneously catalyzed by palladium-based systems containing phosphorus- (P−P) or nitrogen-donor chelating ligands (N−N), in the presence of different cocatalysts (usually Brønsted acids) and/or co-reagents (usually quinones).[5] While in this reaction P-donor ligands are better suited for aliphatic α-olefins, the catalysts of choice for vinyl

* To whom correspondence should be addressed. E-mail: milani@dsch.univ.trieste.it.

(1) (a) Fache, F.; Schulz, E.; Tommasino, M. L.; Lemaire, M. *Chem. Rev.* **2000**, *100*, 2159. (b) Togni, A.; Venanzi, L. M. *Angew. Chem., Int. Ed. Engl.* **1994**, *33*, 497.

(2) Chelucci, G.; Thummel, R. P. *Chem. Rev.* **2002**, *102*, 3129.

(3) (a) Coates, G. W.; Hustad, P. D.; Reinartz, S. *Angew. Chem., Int. Ed.* **2002**, *41*, 2236. (b) Coates, G. W.; Tian, J. *Angew. Chem., Int. Ed.* **2000**, *39*, 3626.

(4) Catalytic Synthesis of Alkene-Carbon Monoxide Copolymers and Cooligomers. In *Catalysis by Metal Complexes*; Sen, A., Ed.; Kluwer Academic Publisher: Dordrecht, 2003.

10.1021/om0493412 CCC: $27.50
Publication on Web 10/13/2004

arenes are based on N-donor ligands.[6] More recently, CO/styrene and CO/substituted styrene copolymers have been obtained even with hybrid P−N[7] or phosphino-phosphite (P−OP) derivatives.[8]

The stereochemistry of these polyketones is basically dictated by the symmetry of the N−N ligand. As a general rule, C_{2v} symmetry ligands, such as 1,10-phenanthroline (phen) and 2,2′-bipyridine (bpy), lead to syndiotactic polyketones,[9,10] while enantiomerically pure C_2 symmetry ligands, such as bisoxazolines and diketimines, give optically active, isotactic copolymers.[11−13] Instead, when C_s or C_1 ligands are used, the stereoselectivity is hardly envisionable and polymers featuring all the possible different stereoregularities can be obtained.[7,14−16]

The main problem encountered with these catalytic systems is related to the low stability of the active species, which can easily undergo decomposition to inactive palladium metal, thus precluding the possibility to obtain the corresponding polyketones in high yield and in high molecular weight.

Our efforts in this field of research have been mainly addressed to the CO/styrene copolymerization reaction promoted by Pd(II) complexes with two molecules of nitrogen-donor chelating ligand, $[Pd(N-N)_2][X]_2$ (N−N = bpy, phen, and their symmetrically substituted derivatives; X = PF_6^-, BF_4^-, CF_3COO^-, triflate (OTf), tosylate (OTs)).[9,17] In previous studies, we found that these catalyst precursors are very sensitive to the nature of the medium and that a change of the solvent from methanol to 2,2,2-trifluoroethanol (TFE) resulted in a remarkable increase of stability of the active species and in a productivity up to 17 kg CP/g Pd.[9a] Thanks to the improved stability of the catalyst, the copolymerization can be performed also in the absence of any oxidant (usually 1,4-benzoquinone, BQ), and this results in a further increase of the molecular weight of the copolymers up to a value of 88 000.[9b] MALDI-TOF analysis of the polyketones synthesized in trifluoroethanol evidenced that only unsaturated end-groups are present in the polymers, thus indicating that β-hydrogen elimination is the unique termination process.

Several years ago some of us found that rhodium complexes with 1,10-phenanthroline substituted in position 3 by a chiral alkyl group (3-R*-phen) display excellent catalytic activities and provide good stereoselectivities in the Rh-catalyzed asymmetric H-transfer reduction from propan-2-ol to acetophenone, the best results being obtained with (*S*)-3-(1,2,2-trimethylpropyl)-1,10-phenanthroline (3-tmp-phen).[18]

In a recent preliminary communication we reported that in the CO/styrene and CO/*p*-Me-styrene copolymerization reactions the bischelated complex with 3-tmp-phen, $[Pd(3\text{-tmp-phen})_2][PF_6]_2$, affords the corresponding polyketones in high yields and with an unprecedentedly high molecular weight (up to 300 000).[16] These positive results prompted us to address a systematic investigation on the coordination chemistry of a range of 3-R-phen to palladium and on their catalytic behavior in copolymerization reactions. In this paper we report the results of this investigation.

Results and Discussion

Synthesis and Characterization of Pd Complexes $[Pd(3\text{-R-phen})_2][PF_6]_2$ 2a−7a. The 3-R-phen studied (Chart 1), namely, 3-Me-phen (**2**), 3-Et-phen (**3**), 3-*i*Pr-phen (**4**), 3-*n*Bu-phen (**5**), 3-*s*Bu-phen (**6**), and 3-tmp-phen (**7**), are characterized by the presence of alkyl groups of different length and steric demand on the heterocyclic rings. Their syntheses were performed following the procedures reported in the literature,[19] with yields ranging from 10% to 60%. The ^{1}H NMR spectra of 3-R-phen show that the signals related to protons of the substituted N-ring (H^2 and H^4) are upfield shifted with respect to the same signals for phen, in agreement with the +I effect of the alkyl group in position 3. The signals of all the other protons are unaffected by the presence of the substituent. No significant variation of the chemical shifts is observed upon changing the R group.

Synthesis of the Dicationic Bischelated Pd(II) Complexes $[Pd(3\text{-R-phen})_2][PF_6]_2$, 2a−7a, this was performed starting from palladium acetate following two different procedures developed by us some years ago (Scheme 1).[9a,20] The two-step pathway (Scheme 1, part a), which implies the isolation of the monochelated derivative $[Pd(CF_3COO)_2(N-N)]$, was applied in all

(5) (a) Sen, A.; Lai, T. W. *J. Am. Chem. Soc.* **1982**, *104*, 3520. (b) Drent, E.; Budzelaar, P. H. M. *Chem. Rev.* **1996**, *96*, 663. (c) Nozaki, K.; Hiyama, T. *J. Organomet. Chem.* **1999**, *576*, 248. (d) Bianchini, C.; Meli, A. *Coord. Chem. Rev.* **2002**, *225*, 35. (e) Mul, W. P.; van der Made, A. W.; Smaardijk, A. A.; Drent, E. In *Catalytic Synthesis of Alkene-Carbon Monoxide Copolymers and Cooligomers*; Sen, A., Ed.; Kluwer Academic Publisher: Dordrecht, 2003; Chapter 4, p 87.

(6) (a) Drent, E. Eur. Pat. Appl. 229408, 1986 (*Chem. Abstr.* **1988**, *108*, 6617). (b) Barsacchi, M.; Consiglio, G.; Medici, L.; Petrucci, G.; Suter, U. W. *Angew. Chem., Int. Ed. Engl.* **1991**, *30*, 989. (c) Pisano, C.; Mezzetti, A.; Consiglio, G. *Organometallics* **1992**, *11*, 20.

(7) (a) Sperrle, M.; Aeby, A.; Consiglio, G.; Pfaltz, A. *Helv. Chim. Acta* **1996**, *79*, 1387. (b) Aeby, A.; Bangerter, F.; Consiglio, G. *Helv. Chim. Acta* **1998**, *81*, 764. (c) Aeby, A.; Gsponer, A.; Consiglio, G. *J. Am. Chem. Soc.* **1998**, *120*, 11000. (d) Aeby, A.; Consiglio, G. *Inorg. Chim. Acta* **1999**, *296*, 45. (e) Gsponer, A.; Consiglio, G. *Helv. Chim. Acta* **2003**, *86*, 2170.

(8) (a) Nozaki, K.; Sato, N.; Takaya, H. *J. Am. Chem. Soc.* **1995**, *117*, 9911. (b) Nozaki, K.; Komaki, H.; Kawashima, Y.; Hiyama, T.; Matsubara, T. *J. Am. Chem. Soc.* **2001**, *123*, 534. (c) Iggo, J. A.; Kawashima, Y.; Liu, J.; Hiyama, T.; Nozaki, K. *Organometallics* **2003**, *22*, 5418.

(9) (a) Milani, B.; Anzilutti, A.; Vicentini, L.; Sessanta o Santi, A.; Zangrando, E.; Geremia, S.; Mestroni, G. *Organometallics* **1997**, *16*, 5064. (b) Milani, B.; Corso, G.; Mestroni, G.; Carfagna, C.; Formica, M.; Seraglia, R. *Organometallics* **2000**, *19*, 3435.

(10) (a) Barsacchi, M.; Batistini, A.; Consiglio, G.; Suter, U. W. *Macromolecules* **1992**, *25*, 3604. (b) Carfagna, C.; Gatti, G.; Martini, D.; Pettinari, C. *Organometallics* **2001**, *20*, 2175.

(11) Brookhart, M.; Wagner, M. I.; Balavoine, G. G. A.; Haddou, H. A. *J. Am. Chem. Soc.* **1994**, *116*, 3641.

(12) (a) Bartolini, S.; Carfagna, C.; Musco, A. *Macromol. Rapid Commun.* **1995**, *16*, 9. (b) Binotti B.; Carfagna, C.; Gatti, G.; Martini, D.; Mosca L.; Pettinari, C. *Organometallics* **2003**, *22*, 1115.

(13) Reetz, M. T.; Aderlein, G.; Angermund, K. *J. Am. Chem. Soc.* **2000**, *122*, 996.

(14) (a) Sen, A.; Jiang, Z. *Macromolecules* **1993**, *26*, 911. (b) Bastero, A.; Ruiz, A.; Reina, J. A.; Claver, C.; Guerrero, A. M.; Jalon, F. A.; Manzano, B. R. *J. Organomet. Chem.* **2002**, *619*, 287.

(15) (a) Bastero, A.; Ruiz, A.; Claver, C.; Castillon, S. *Eur. J. Inorg. Chem.* **2001**, 3009. (b) Bastero, A.; Ruiz, A.; Claver, C.; Milani, B.; Zangrando, E. *Organometallics* **2002**, *21*, 5820.

(16) Milani, B.; Scarel, A.; Mestroni, G.; Gladiali, S.; Taras, R.; Carfagna, C.; Mosca, L. *Organometallics* **2002**, *21*, 1323.

(17) Sommazzi, A.; Garbassi, F.; Mestroni, G.; Milani, B. U.S. Patent 5 310 871, 1994.

(18) (a) Gladiali, S.; Pinna, L.; Delogu, G.; De Martin, S.; Zassinovich, G.; Mestroni, G. *Tetrahedron Asymm.* **1990**, *1*, 635. (b) Zassinovich, G.; Mestroni, G.; Gladiali, S. *Chem. Rev.* **1992**, *92*, 1051.

(19) Gladiali, S.; Chelucci, G.; Mudadu, M. S.; Gastaut, M. A.; Thummel, R. P. *J. Org. Chem.* **2001**, *66*, 400.

(20) Milani, B.; Vicentini, L.; Sommazzi, A.; Garbassi, F.; Chiarparin, E.; Zangrando, E.; Mestroni, G. *J. Chem. Soc., Dalton Trans.* **1996**, 3139.

Chart 1. The Studied Phenanthrolines

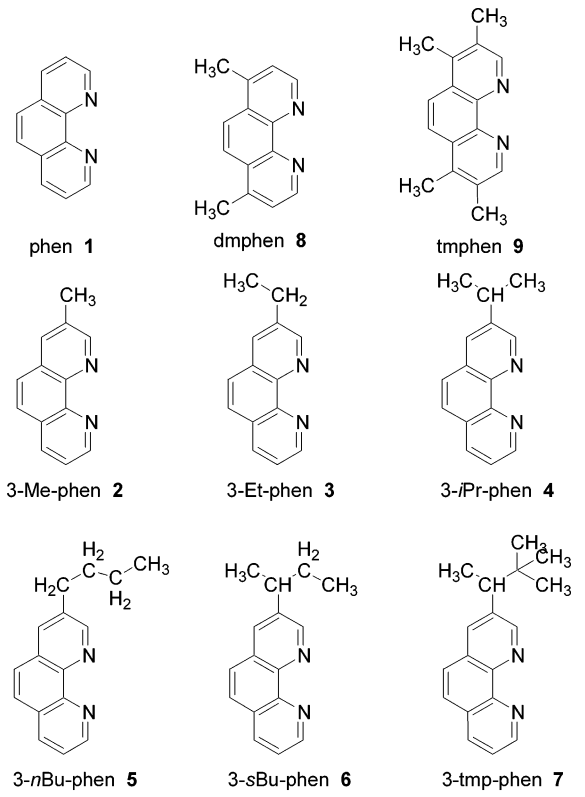

Scheme 1. Synthetic Pathways for Complexes $[Pd(3\text{-R-phen})_2][PF_6]_2$: (a) the Two-Step Procedure for 1a −4a, 6a−9a; (b) the One-Pot Reaction for 5a

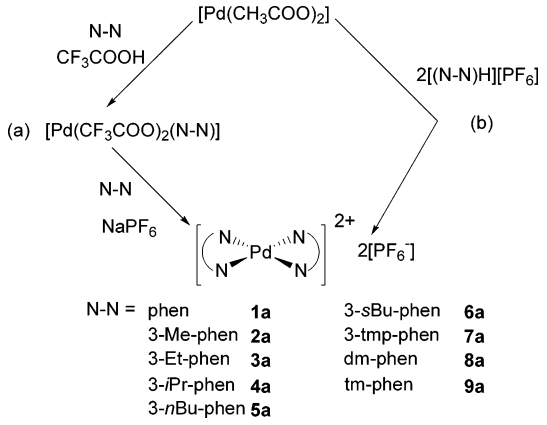

cases except with complex **5a**. This last was synthesized according to the one-pot procedure (Scheme 1, part b), which was more appropriate for a ligand stored in the form of hydrochloride. However, it was necessary to transform the chloride salt $[(3\text{-}n\text{Bu-phen})H_2][Cl]_2$ (**5′**) into the corresponding hexafluorophosphate derivative $[(3\text{-}n\text{Bu-phen})H][PF_6]$ (**5″**) prior to use.

Both synthetic methods led to the isolation of the final products as yellow microcrystalline solids, in high yield and in high purity (see Experimental Section; Table 6). Single crystals suitable for X-ray analysis were obtained for two representatives of this series of complexes, namely, $[Pd(3\text{-}i\text{Pr-phen})_2][PF_6]_2$ (**4a**) and $[Pd(3\text{-}n\text{Bu-phen})_2][PF_6]_2$ (**5a**).

The X-ray structural determination evidences (Figures 1 and 2) the palladium atom located on a crystallographic 2-fold axis with Pd−N distances of 2.060(3) and 2.026(3) Å in **4a** and 2.037(5) and 2.021(5) Å in **5a**.

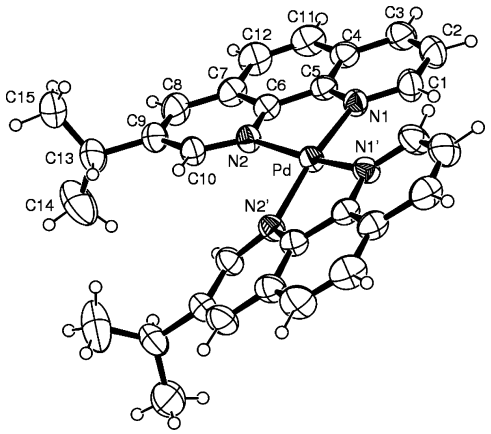

Figure 1. Molecular structure of the cation of **4a** (thermal ellipsoids at 40% probability level). Of the disordered *i*-Pr groups, only atoms at higher occupancy (0.64%) are indicated for the sake of clarity. Selected bond distances (Å) and angles (deg): Pd−N(1) 2.060(3), Pd−N(2) 2.026(3), N(2)−Pd−N(1) 80.38(13), N(2)−Pd−N(1′) 167.45(13), N(1)−Pd−N(1′) 104.1(2), N(2′)−Pd−N(2) 97.8(2). Primed atoms at $-x+1, y, -z+3/2$.

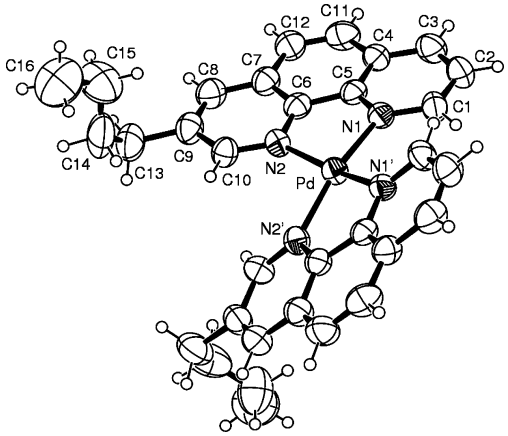

Figure 2. Molecular structure of the cation of **5a** (thermal ellipsoids at 40% probability level). Of the disordered *n*-Bu groups only atoms at higher occupancy (0.66%) are reported. Selected bond distances (Å) and angles (deg): Pd−N(1) 2.037(5), Pd−N(2) 2.021(5), N(2)−Pd−N(1) 81.1(2), N(2)−Pd−N(1′) 164.9(2), N(1′)−Pd−N(1) 102.3(3), N(2)−Pd−N(2′) 99.4(3). Primed atoms at $-x+1, y, -z+3/2$.

These distances, which show shorter values for the nitrogen close to the alkyl group, suggesting a more basic site, are fairly comparable in **5a**, but are significantly different in **4a** (difference of ca. 11σ).

The square planar coordination geometry is tetrahedrally distorted toward a *twist* conformation, which represents one of the distinctive solid state arrangements, found in bis(bpy) and bis(phen) species.[21] This distortion relieves the steric interactions between the hydrogen atoms close to the nitrogen donors, giving rise to a C_2 symmetry chiral complex. The two phen units are assembled in a *syn* arrangement, i.e., with the alkyl groups located on the same side of the square planar geometry. The chiral complexes belong to a centrosymmetric space group indicating the formation of racemic mixtures.

(21) A second type of distortion was indicated as *bow-step*: Geremia, S.; Randaccio, L.; Mestroni, G.; Milani, B. *J. Chem. Soc., Dalton Trans.* **1992**, 2117.

Table 1. Selected ^{1}H NMR Data for Ligands 3-R-phen 2−7 and Related Pd(II) Complexes 2a−7a: Region of Aliphatic Protons[a]

ligand/complex	CH_2 α	CH_2 β	CH_2 γ	CH	CH_3
3-Me-phen **2**					2.60 (3H, s)
2a					2.81 (6H, s)
3-Et-phen **3**	2.92 (2H, q)				1.39 (3H, t)
3a	3.17 (4H, q)				1.44 (6H, t)
3-*i*Pr-phen **4**				3.23 (1H, m)	1.43 (6H, d)
4a				3.52 (2H, m)	1.48 (12H, d)
3-*n*Bu-phen **5**[b]	2.89 (2H, t)	1.75 (2H, m)	1.44 (2H, m)		0.98 (3H, t)
5a	3.12 (4H, t)	1.82 (4H, m)	1.45 (4H, m)		0.97 (6H, t)
3-*s*Bu-phen **6**		1.77 (2H, m)		2.93 (1H, m)	0.89 (3H, t); 1.41 (3H, d)
6a		1.85 (4H, m)		3.24 (2H, m)	0.91 (6H, t); 1.47 (6H, d)
3-tmp-phen **7**				2.89 (1H, q)	0.95 (9H, s) 1.43 (3H, d)[c]
7a				3.19 (2H, q)	0.94 (18H, s)
					1.47 (6H, d)

[a] ^{1}H NMR spectra were recorded in $CDCl_3$ for the ligands and in DMSO-d_6 for the complexes, at room temperature; s = singlet, d = doublet, t = triplet, q = quartet, m = multiplet; δ values are in ppm. [b] Spectrum recorded dissolving the brown oil. [c] CH_3 signal bound to CH.

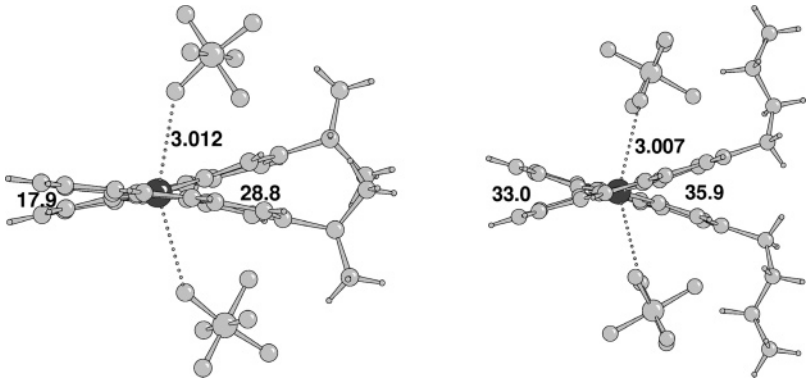

Figure 3. *Twist* conformation in complexes **4a** and **5a** indicating the Pd−F distances (Å) and the dihedral angles (deg) between facing py rings.

This *syn* arrangement is similar to the one previously reported in a series of organometallic bis-homoleptic platinum complexes with N−C aromatic ligands,[22] where the geometry detected in the solid state is consistently *cis*. This disposition corresponds to the thermodynamically more stable geometry of the complexes because it prevents two *trans* effecting C atoms from competing with each other.

The extent of the tetrahedral distortion in the present complexes is measured by the interplanar angle between the Pd/N(1)/N(2) planes, which is 18.9(1)° and 23.2(2)°, in **4a** and **5a**, respectively. Upon binding, the two phen ligands undergo a slight distortion from the original planarity. As a consequence, the calculated dihedral angles between facing pyridine rings are different, being wider on the side of the alkyl groups (Figure 3). The difference between these dihedral angles is a measure of the phen ligand distortion. While in **5a** this difference is small, it is more pronounced in the case of the more sterically demanding isopropyl-substituted ligand (Figure 3).

The molecular packing shows weak interactions between the metal and the counterion with Pd- -F distances of about 3.0 Å (Figure 3). This feature, which might have some bearing on the catalytic behavior, is not novel in the solid state, and formation of ion pairs for similar complexes was demonstrated also in solution via NMR studies.[23]

The characterization in solution of complexes **1a**−**7a** was made by ^{1}H NMR spectroscopy, recording the spectra in DMSO-d_6 solution, at room temperature. The chemical shifts of the aliphatic protons are listed in Table 1. General features of the spectra are as follows: (i) all the signals are shifted to high frequency with respect to the free ligand; (ii) no signal due to free ligand is present. From these facts and from the number of signals and their integration, it is concluded that the two molecules of 3-R-phen are equivalent and bound to palladium. While these ^{1}H NMR data are in agreement with the *syn* coordination geometry observed in the solid state, they do not rule out the *anti* geometry.

Broad signals are observed at room temperature in the ^{1}H NMR spectrum of the complex $[Pd(3\text{-}i\text{Pr-phen})_2][PF_6]_2$. Addition of variable amounts (0.5−2 equiv) of 3-*i*Pr-phen to the solution resulted in a progressive shift of all the signals to lower frequencies. In no case, however, could the resonances of the free ligand be detected. These experiments indicate that in solution an equilibrium of exchange between bound and free 3-R-phen is occurring and that its rate is in the range of the NMR time scale.[9a]

(22) (a) Chassot, L.; Muller E.; von Zelewsky, A. *Inorg. Chem.* **1984**, *23*, 4249. (b) Jolliet, P.; Gianini, M.; von Zelewsky, A.; Bernardinelli, G.; Stoeckli-Evans, H. *Inorg. Chem.* **1996**, *35*, 4883. (c) Gianini, M.; Forster, A.; Haag, P.; von Zelewsky, A.; Stoeckli-Evans, H. *Inorg. Chem.* **1996**, *35*, 4889.

(23) Macchioni, A.; Bellachioma, G.; Cardaci, G.; Travaglia, M.; Zuccaccia, C.; Milani, B.; Corso, G.; Zangrando, E.; Mestroni, G.; Carfagna, C.; Formica, M. *Organometallics* **1999**, *18*, 3061.

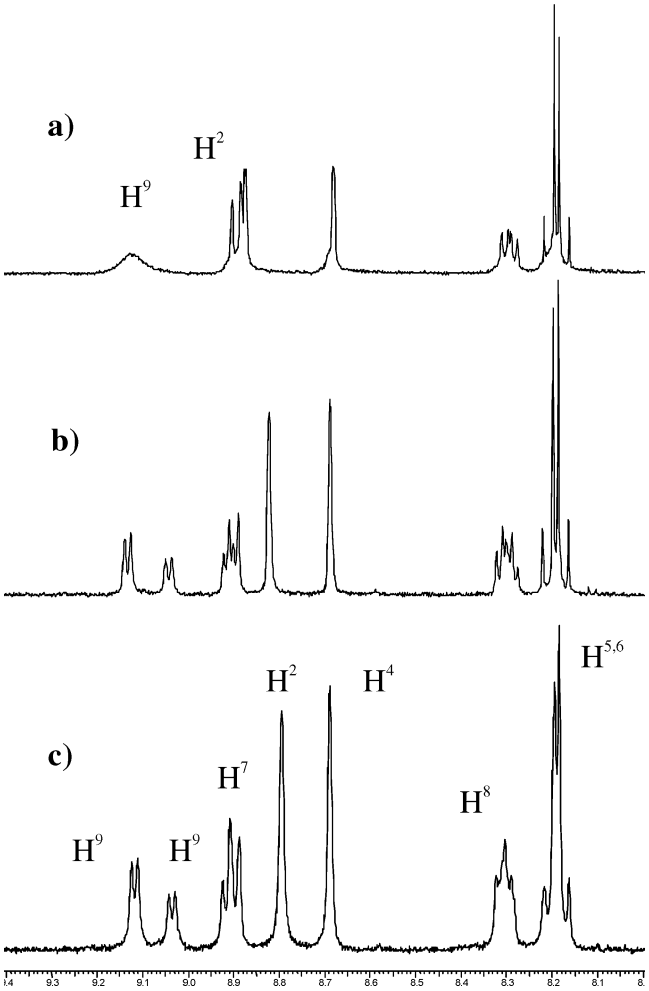

Figure 4. ^{1}H NMR spectra of **5a** in CD_2Cl_2, region of aromatic protons. Variations with temperature: (a) T = 25 °C; (b) T = −40 °C; (c) T = −80 °C.

The solubility of complex **5a** in CD_2Cl_2 allowed for the evolution of this process to be monitored by NMR at low temperature. A dynamic behavior was readily noticed and, for instance, the H^9 resonance, broad at room temperature, is split into two signals of different intensity at −80 °C (Figure 4). Although most of the split signals could not be isolated, the pattern of the spectrum is indicative of the presence of no more than two species. As no resonance conceivably attributable to the free ligand could be observed, in both of them the ligand must be present in the bound state and should experience a similar chemical environment. An NOE experiment, performed at T = −40 °C, based on irradiation of the doublet at 9.03 ppm, confirmed that the two species are in equilibrium and evidenced an NOE effect between H^9 and H^2 (the singlet at 8.83 ppm), in addition to the expected NOE between H^9 and H^8. The same results are obtained when the doublet at 9.11 ppm was irradiated. The presence of the NOE effect between H^9 and H^2 indicates that these two protons are close to each other, and this is possible only in the *anti* isomer. Therefore, we conclude that the dynamic process is the equilibrium between *syn* and *anti* isomers of the starting complex (Scheme 2).

Theoretical Analysis. To rationalize some surprising structural features and to assess the electronic structure of the Pd complexes, in particular the relation

Scheme 2. Equilibrium between *syn* and *anti* Isomers for Complexes $[Pd(3\text{-}R\text{-}phen)_2][PF_6]_2$

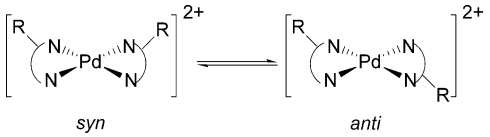

syn *anti*

with the effect of the alkyl substitution of the coordinated ligand on the electron density of the complex, a series of density functional theory (DFT) calculations have been carried out. The optimized geometries have been calculated for the Pd complex **1a**, for the *syn* and *anti* isomers of **4a** and **5a**, and for $[Pd(tmphen)_2][PF_6]_2$, **9a** (tmphen = 3,4,7,8-tetramethyl-1,10-phenanthroline), as well as for the relevant free ligands. The geometry optimizations have been supplemented with an analysis of the Mulliken charges and of the eigenvalues of core electrons to gain more information on the changes of the electron density distribution due to the different R groups. The results are collected in Table 2, together with the experimental values of the Pd−N distances.

The agreement between the calculated and the experimental Pd−N distances for the *syn* complex **4a** is quite good. The Pd−N(2) distance between the metal and the N atom proximal to the R alkyl group of the ligand is found to be shorter than the Pd−N(1) distance, and the discrepancies with respect to the experiment are lower than 0.004 Å. Since it is expected that steric effects should act in the opposite direction, this somehow surprising result suggests that electronic effects are the actual origin of the observed structural trends.

For the *syn* complex **5a** the same effect is found, but is less pronounced in both calculated and experimental results. It is worth noting that for the *anti* isomers the differences are much less evident.

To assess the effect of the R groups on the electron density, the Mulliken charges have been reported as well in Table 2. If the *syn* complex **4a** is considered first, it is apparent that the N(1) ligand atom is more negative by about 0.04 e^- than the N(2) one, which is in contrast with what is expected from the R electron-donor effect. As an alternative to Mulliken charges, which are strongly basis set dependent, core electron eigenvalues may be employed to gain qualitative information on the charge distribution.[24] The comparison between the core eigenvalues of the different complexes is much more informative: in fact while N 1s of N(1) and N(2) of **4a** and **5a** are very similar, for **1a** a stabilization of about 0.4 eV and for $[Pd(tmphen)_2]^{2+}$ a destabilization of 0.5 eV are found. This indicates that on the N atoms of the coordinated ligands the lowest electron charge is found in **1a**, while the largest one is in $[Pd(tmphen)_2]^{2+}$, and **4a** and **5a** lie between, in agreement with the expected R electron-donor property. It is interesting to observe that the same trend is found for the free ligands, although somewhat less pronounced. A supplement of information is given by the Pd 1s eigenvalues: in this case the most stable (negative) one is relative to the **1a** complex, which therefore carries the most positive charge in the series, while $[Pd(tmphen)_2]^{2+}$ appears to be the most destabilized and therefore the less positively

(24) Haberlen, O. D.; Chung, S. C.; Stener, M.; Rösch, N. *J. Chem. Phys.* **1997**, *106*, 5189.

Table 2. DFT Calculated Properties for *syn* and *anti* 4a and 5a, 1a Pd Complexes, and Free Ligands, and for tmphen Complex and Free Ligand[a]

	4a			**5a**						
	syn	*anti*	**4**	*syn*	*anti*	**5**	**9a**	tmphen	**1a**	**1**
d Pd−N(2)	2.022 (exptl 2.026)	2.043		2.035 (exptl 2.021)	2.075		2.040 (exptl 2.036)		2.037 (exptl 2.017)	
d Pd−N(1)	2.058 (exptl 2.060)	2.052		2.041 (exptl 2.037)	2.078					
Q N(2)	−0.395	−0.397	−0.225	−0.399	−0.396	−0.217	−0.411	−0.232	−0.420	−0.240
Q N(1)	−0.434	−0.411	−0.241	−0.423	−0.416	−0.242				
Q Pd	+1.182	+1.165		+1.180	+1.098		+1.143		+1.188	
ϵ(1s) N(2)	−386.32	−386.24	−378.04	−386.28	−386.26	−378.05	−385.71	−377.77	−386.66	−378.15
ϵ(1s) N(1)	−386.29	−386.31	−378.05	−386.29	−386.29	−378.05				
ϵ(1s) Pd	−23412.24	−23412.22		−23412.22	−23412.15		−23411.71		−23412.60	
ΔBE	0.00	+0.55		0.00	+5.58					

[a] Relevant distances (*d*, in Å), Mulliken charges (*Q*, in e$^-$), core eigenvalues (ϵ, in eV), and relative binding energies with respect to the most stable isomer (ΔBE, in kcal/mol).

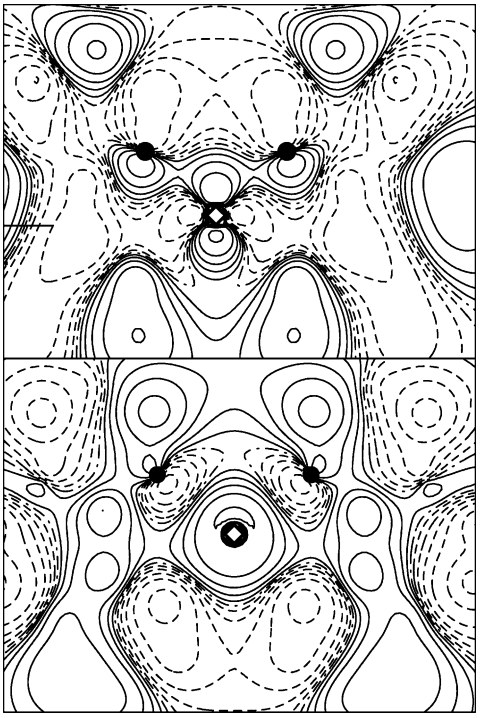

Figure 5. Contour plot of the HOMO *syn* **4a** orbital: solid, dashed, and dot−dashed lines indicate positive, negative, and zero (nodal) contribution; solid circles N atoms, hollow diamond Pd atom. Upper panel: HOMO plotted over the plane that contains Pd and two N(2) atoms. Lower panel: HOMO plotted over the plane that contains Pd and two N(1) atoms.

charged. These findings show that the overall consequence of the alkyl substitution on the ligands is an increase of the negative charge on the N atoms and a decrease of the positive charge on the metal.

The surprisingly short Pd−N(2) distance, calculated and measured for the sterically less favored *syn* **4a** complex, has suggested a more detailed analysis of the electronic structure of this compound, in order to identify an electronic effect, which may act in the opposite direction of the steric one. In Figure 5 the HOMO orbital for **4a** is represented as isolines over proper planes: solid, dashed, and dot−dashed curves indicate positive, negative, and zero (nodal) contribution of the wave function. In the upper panel, the plane is chosen in order to contain two N(2) and Pd atoms: it is apparent that the interaction among these three centers is of bonding character; in fact there is an overlap with the same sign between the metal and the N atoms. On the other hand, in the lower panel the HOMO is considered over the plane containing the Pd and the N(1) atoms: in this case a change of sign is evident between the metal and the N atoms, which indicates an interaction of antibonding character. So we are led to attribute the shorter Pd−N(2) distance to an electronic effect, which is of bonding character at variance with the Pd−N(1) interaction, which is antibonding. We have also investigated the presence of direct ligand−ligand interaction. In Figure 6 the HOMO orbital has been considered in two different planes: in the upper panel, the plane is chosen perpendicular to the molecular average plane, but passing through the C(10) atoms of the ligand fragments, which are contiguous to the N(2) atoms. An evident bonding interaction is found directly between the C(10) atoms, mediated by 2p C orbitals, which belong to the phenanthroline π system. On the other hand, a much less effective bonding overlap is found when the plane containing the C(1) atoms (lower panel) in the opposite direction with respect to the R substituent is considered. Therefore, it is worth noting that the bonding interaction is possible because the two planes of the two ligands are slightly opened in the direction of the R substituent. We can summarize these findings saying that for this complex the electronic effects play a double role: the Pd−N distance trend is an effect of the interplay between bonding and antibonding character, while the opening between the ligand rings operated by the steric substitution induces a favorable bonding interaction between the ligand π systems.

To gain some information on the isomer relative stabilities, we have computed the energy differences between the *syn* and the *anti* isomers of **4a** and **5a**: in both cases the *syn* isomer is calculated as the most stable (Table 2). For **4a** the difference is very small (only 0.55 kcal/mol), so we can expect similar stability for the two isomers, while for **5a** a Stefan−Boltzmann distribution gives a clear-cut preference for the *syn* isomer. In agreement with this suggestion, the NMR investigation at low temperature evidences the presence, in solution, of two species: the *syn* and *anti* isomers.

Copolymerization Reactions. The copolymerization tests were carried out in trifluoroethanol with no addition of any cocatalyst or co-reagent, at different temperatures and pressures depending on the nature of the olefin. The solids isolated at the end of the runs

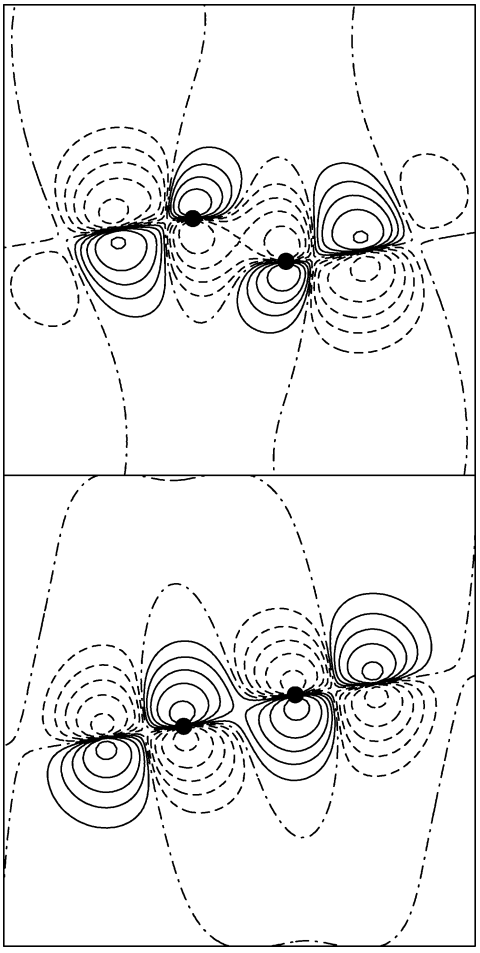

Figure 6. Contour plot of the HOMO *syn* **4a** orbital: solid, dashed, and dot−dashed lines indicate positive, negative, and zero (nodal) contribution; solid circles C atoms. Upper panel: HOMO plotted over the plane perpendicular to the average molecular plane and containing C(10) atoms. Lower panel: HOMO plotted over the plane perpendicular to the average molecular plane and containing C(1) atoms.

Table 3. CO/Styrene Copolymerization: Effect of Nitrogen-Donor Ligand (Catalyst Precursor: [Pd(N−N)$_2$][PF$_6$]$_2$[a])

N−N	pK_a	g CP	kg CP/g Pd
phen (**1a**)	4.86	0.86	1.50
dmphen (**8a**)	5.94	0.45	0.78
tmphen (**9a**)	6.31	traces	n.d.

[a] Reaction conditions: $n_{Pd} = 0.54 \times 10^{-5}$ mol; solvent TFE $V =$ 20 mL; styrene $V = 30$ mL; $T = 50$ °C; $P_{CO} = 40$ atm; $t = 24$ h, [styrene]/[Pd] = 48 000.

are perfectly alternating CO/olefin polyketones, as apparent from their characterization.[20,25]

As reference data the catalytic behavior in CO/styrene copolymerization reaction of bischelated complexes with C_{2v} symmetry ligands was studied. On going from phen to 4,7-dimethyl-1,10-phenanthroline (dmphen) and to 3,4,7,8-tetramethyl-1,10-phenanthroline, a progressive decrease of productivity was observed, and in particular, when the complex [Pd(tmphen)$_2$][PF$_6$]$_2$ was used, only traces of polymer were obtained (Table 3). In all cases no decomposition of the active species to palladium metal was observed, thus indicating that the loss of activity is related to the inertness of the precatalyst and not to the instability of the catalyst. An analogous trend has been already reported by us[26] and others[27] for the CO/styrene copolymerization promoted by monochelated complexes, [Pd(CH$_3$COO)$_2$(N−N)] and [Pd(CF$_3$COO)$_2$-(N−N)], and for the CO/ethylene copolymerization promoted by the bischelated derivatives [Pd(dppp)-(N−N)][PF$_6$]$_2$, in methanol.[20] However, in the present study the influence of the N−N ligand is definitely more pronounced than previously observed.

Table 4. CO/Styrene Copolymerization: Effect of the Alkyl Substituent (Catalyst Precursor: [Pd(3-R-phen)$_2$][PF$_6$]$_2$[a])

run	3-R-phen (catalyst)	g CP	kg CP/g Pd	$\langle M_w \rangle$ ($\langle M_w \rangle/\langle M_n \rangle$)	R.U.[b]
1	phen (**1a**)	0.86	1.50	108 000 (1.86)	818
2	3-Me-phen (**2a**)	0.63	1.10	104 000 (1.85)	787
3	3-Et-phen (**3a**)	0.90	1.57	124 000 (1.81)	938
4	3-*i*Pr-phen (**4a**)	1.15	2.00	151 000 (1.62)	1143
5	3-*n*Bu-phen (**5a**)	1.22	2.12	149 000 (1.86)	1128
6	3-*s*Bu-phen (**6a**)	1.24	2.16	147 000 (1.56)	1113
7	3-tmp-phen (**7a**)	1.53	2.66	206 000 (1.54)	1559

[a] Reaction conditions: see Table 3. [b] R.U. = number of repetitive units inserted in the polymeric chain.

The origin of the ligand effect correlates well with the variation of the electron charge present on the N atoms of ligands and on palladium, as evidenced by the theoretical analysis. Changing phen with tmphen results in a decrease of the positive charge on palladium, which becomes less electrophilic, and this fact can account for the comparably lower activity displayed by the tmphen monochelated complex with respect to the phen derivative. At the same time, as the electron density on the N atoms increases from phen to tmphen, the strength of the Pd−N bond increases, and opening of one chelate ring through dissociation of a N-donor becomes more difficult. Since the lack of activity of the [Pd(tmphen)$_2$][PF$_6$]$_2$ complex is reasonably related to this strengthening, we may infer that vacation of a coordination site of the starting complex by cleavage of one Pd−N bond in an early step of the copolymerization should be required and that this process is suppressed when the Pd−N bond becomes stronger.

The bischelated complexes containing 3-R-phen, [Pd-(3-R-phen)$_2$][PF$_6$]$_2$ **2a**−**7a**, were tested in CO/styrene copolymerization by carrying out the reactions under the same conditions used for complexes [Pd(N−N)$_2$]-[PF$_6$]$_2$, reported in Table 3. The results are compared with the data obtained with **1a**. The introduction in position 3 of the N ligand of a small alkyl group, such as methyl or ethyl, had almost no effect on either the productivity or the molecular weight of the polyketones obtained (Table 4, runs 1−3). Surprisingly, with heavier and/or more hindered substituents, an increase of productivity was found, which is matched by an increase of the molecular weight values (Table 4, runs 4−7). Indeed, CO/styrene polyketones with M_w higher than 100 000 were synthesized for the first time. In all cases no formation of palladium metal was evident, thus

(25) Milani, B.; Alessio, E.; Mestroni, G.; Zangrando, E.; Randaccio, L.; Consiglio, G. *J. Chem. Soc., Dalton Trans.* **1996**, 1021.

(26) Milani, B.; Alessio, E.; Mestroni, G.; Sommazzi, A.; Garbassi, F.; Zangrando, E.; Bresciani-Pahor, N.; Randaccio, L. *J. Chem. Soc., Dalton Trans.* **1994**, 1903.

(27) Santi, R.; Romano, A. M.; Garrone, L.; Abbondanza, L.; Scalabrini, M.; Bacchilega, G. *Macromol. Chem. Phys.* **1999**, *200*, 25.

Table 5. CO/Styrene and CO/*p*-Me-styrene Copolymerization: Effect of the Alkyl Substituent (Catalyst Precursor: [Pd(3-R-phen)$_2$][PF$_6$]$_2$[a])

3-R-phen	CO/styrene R.U.[b]	CO/styrene TON[c]	CO/*p*-Me-styrene R.U.[b]	CO/*p*-Me-styrene TON[c]
t = 24 h				
phen	818	1.27	733	3.43
3-*s*Bu-phen	1242	1.04	938	2.81
3-tmp-phen	1614	1.25	1349	2.89
t = 48 h				
phen	1114	1.71	1096	3.59
3-*s*Bu-phen	1566	1.29	1157	3.40
3-tmp-phen	2045	1.85	1979	2.97
t = 72 h				
phen	1151	2.02	1171	5.07
3-*s*Bu-phen	1636	2.26	1404	3.78
3-tmp-phen	2348	2.62	2151	3.99

[a] Reaction conditions: see Figure 7. [b] R.U. = number of repetitive units inserted in the polymeric chain. [c] TON calculated as mole of copolymer per mole of Pd.

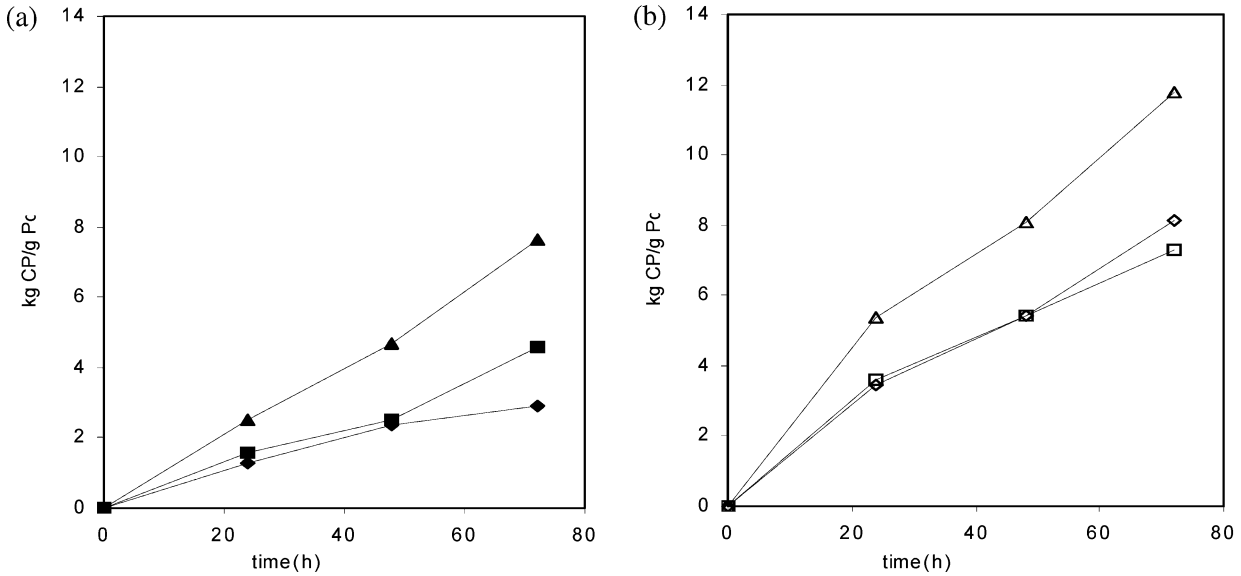

Figure 7. CO/aromatic olefin copolymerization: effect of time on productivity. The catalyst precursor was **1a**, **6a**, or **7a**. Reaction conditions: see Table 3; $n_{Pd} = 0.27 \times 10^{-5}$ mol, [olefin]/[Pd] = 96 000. (a) CO/styrene copolymerization: (◆) phen; (■) 3-*s*Bu-phen; (▲) 3-tmp-phen. (b) CO/*p*-Me-styrene copolymerization: (◇) phen; (□) 3-*s*-Bu-phen; (△) 3-tmp-phen.

confirming the high stability of the active species in the fluorinated alcohol. With just one exception (entry 2) the increase in productivity observed in the first 24 h can be accounted for solely by the increase in molecular weight. This result provides a strong indication that the number of polymeric chains initiated by the catalyst is always the same and that the ligand exerts its effect on the propagation rate, which becomes faster when using sterically demanding 3-alkyl-susbtituted phens.

The catalytic behavior of the two best precatalysts, **6a** and **7a**, was studied in more detail, in comparison with complex **1a**. The copolymerization tests were run at a styrene-to-Pd ratio of 96 000, and the effect of longer reaction times was evaluated. The catalysts, originated by the three complexes, are active at least up to 72 h without showing any decomposition to palladium metal (Figure 7a). The productivity increases almost steadily with time, and this enhancement is particularly evident for the catalyst containing 3-tmp-phen. Indeed, the difference between the phen catalyst and the 3-tmp-phen one increases on prolonging the reaction time, while the productivity of the 3-*s*Bu-phen system is comparable to that of phen. The trend of productivity with time is reflected in that of molecular weight (Figure 8), and the maximum value of 300 000 is reached when the 3-tmp-phen system is used.

Parallel increases of productivity and of molecular weight were observed also in the copolymerization of carbon monoxide with *p*-Me-styrene (Figures 7b and 8). In this case, regardless of the ligand, the productivity is nearly doubled as compared with styrene, while molecular weights are similar. From this observation, it seems that in vinyl arene copolymerizations the molecular weight is basically dictated by the catalyst (the ligands in our cases), while the productivity is basically linked to the nature of the substrate. Moreover, when *p*-Me-styrene is used, the number of repetitive units inserted in the polymer chain is always lower than in the styrene-based polymer (Table 5). This means that the improved productivity observed with this substrate is due to an increase of the number rather than of the length of the polymeric chains, as revealed by the differences in the turnover numbers (TON, Table 5), which are definitely lower in the case of styrene. Therefore, the modest increase of electron density on the double bond of the aromatic olefin resulted in an increase of both the initiation and/or propagation and the termination rate.

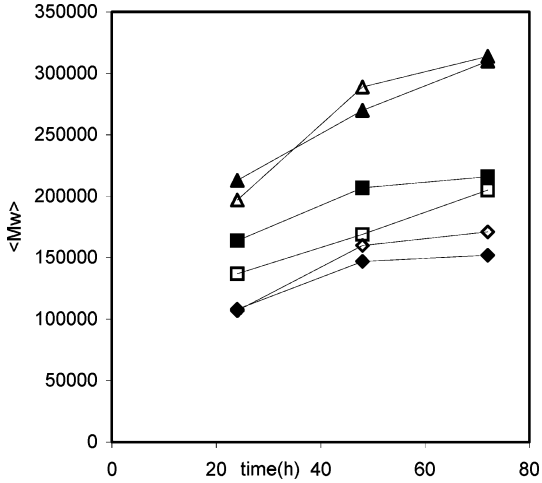

Figure 8. CO/aromatic olefin copolymerization: effect of time on molecular weight. The catalyst precursor was **1a**, **6a**, or **7a**. Reaction conditions: see Figure 7. Legend: (◆) phen, styrene; (◇) phen, *p*-Me-styrene; (■) 3-*s*Bu-phen, styrene; (□) 3-*s*-Bu-phen, *p*-Me-styrene; (▲) 3-tmp-phen, styrene; (△) 3-tmp-phen, *p*-Me-styrene.

It is worth noting that both the productivities and the molecular weight values reached with the 3-tmp-phen catalyst are the highest data ever obtained in these copolymerizations without added oxidant for both styrene and *p*-Me-styrene.

The synthesized CO/aromatic olefins polyketones are mainly syndiotactic (^{13}C NMR characterization) with the usual triad distribution.[16] Therefore, the C_1 symmetry ligands used in the present investigation do not affect the olefin enantioface selection during the polymerization process, which is under chain end control.

Plotting the reaction rate, expressed as productivity per hour, against the time (Figure 9) led us to point out some significant differences in the behavior of the two aromatic olefins. While in the case of CO/styrene copolymerization (Figure 9a) no significant variation was noticed over the range of time monitored, in the case of CO/*p*-Me-styrene copolymerization (Figure 9b), the reaction rate undergoes a sharp decrease between 24 and 48 h, thereafter remaining constant. These differences should be related to the different properties of the relevant polymers. Under our conditions, the CO/styrene copolymer precipitates as a solid in the reactor after only 24 h, whereas the CO/*p*-Me-styrene copolymer remains in homogeneous phase in a solution of increasingly high viscosity up to 48 h and then precipitates. This switch from a homogeneous to a heterogeneous system has obvious effects on the kinetics of the reaction, as previously pointed out in the CO/ethylene copolymerization.[5e] In this reaction at least three different states of the catalyst, one homogeneous and two heterogeneous, can be present at the same time, each of them displaying its own kinetic behavior.

The complexes **1a**−**7a** were also tested in the copolymerization of carbon monoxide with ethylene. The catalytic reactions were carried out always in trifluoroethanol, but in this case, the addition of 1,4-benzoquinone was necessary to avoid fast decomposition of the catalyst. Nevertheless, all the CO/ethylene polyketones synthesized are gray, thus indicating the formation of some palladium metal. Prolonging the reaction time from 16 to 24 h resulted in doubling the productivity (Figure 10), and values around 6 kg CP/g Pd were achieved. In this case the use of 3-R-phen catalyst in place of **1a** did not produce significant differences of productivity. Apparently with ethylene as the substrate, the catalytic activity of the complex is not significantly influenced by the presence of the alkyl group on the phenanthroline.

The molecular weights of the polyketones obtained with **5a** are in the range 50 000. Unlike the case of the aromatic substrates, they do not vary with time (Figure 11).

Overall the results obtained in the CO/ethylene copolymerization evidence that, even if the values of productivity are quite high, they are still lower than those typically obtained with the catalytic systems based on dppp or on its substituted derivatives.[5e] On the other

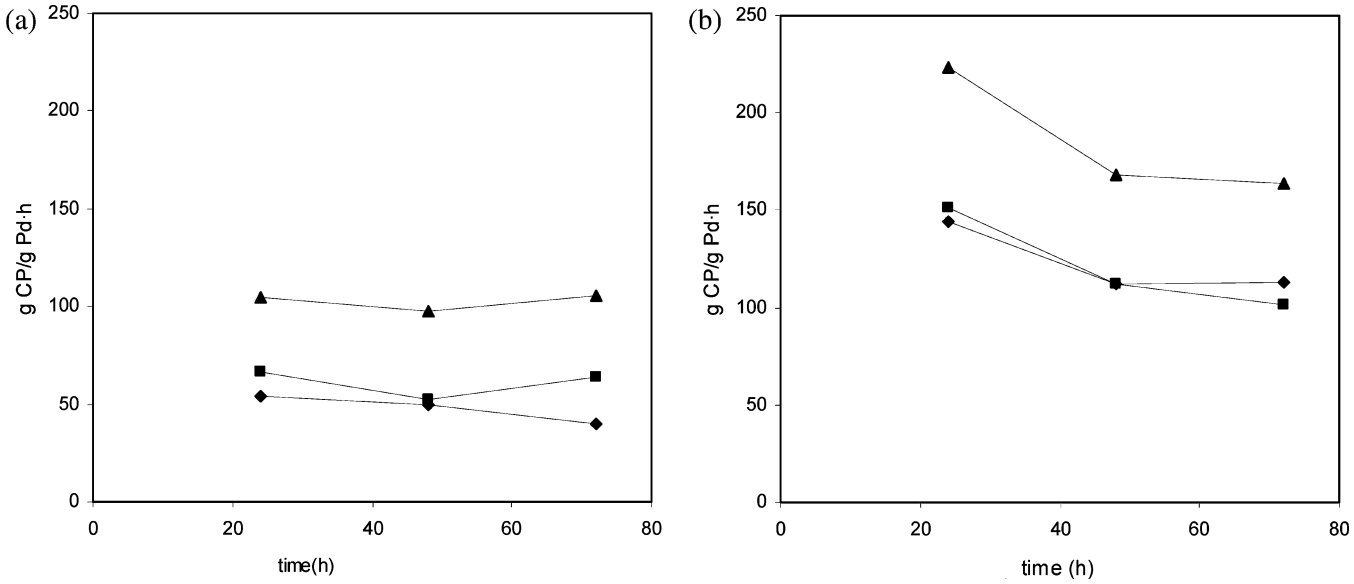

Figure 9. CO/aromatic olefin copolymerization reaction: plot of rate vs time. (a) CO/styrene copolymerization: (■) phen; (▲) 3-*s*Bu-phen; (◆) 3-tmp-phen. (b) CO/*p*-Me-styrene copolymerization: (◆) phen; (■) 3-*s*-Bu-phen; (▲) 3-tmp-phen. Reaction conditions: see Figure 7.

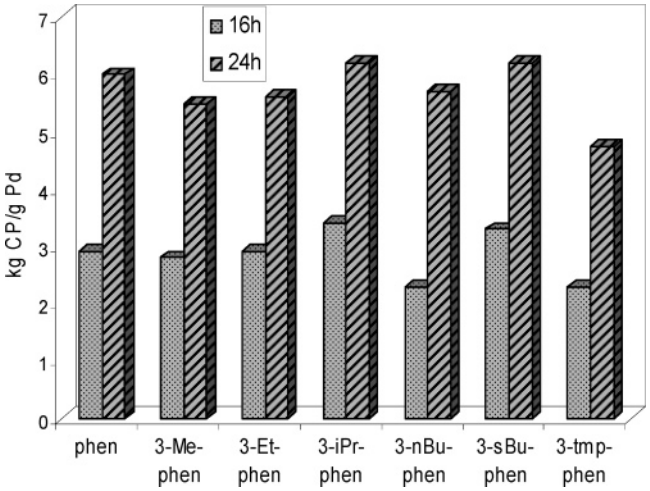

Figure 10. CO/ethylene copolymerization reaction: effect of the alkyl substituent. Catalyst precursor: $[Pd(3\text{-R-phen})_2][PF_6]_2$. Reaction conditions: $n_{Pd} = 5.0 \times 10^{-6}$ mol; solvent TFE $V = 50$ mL; $P_{TOT} = 30$ atm; $CO:C_2H_4 = 1:1$; $T = 70$ °C; [BQ]/[Pd] = 20 for the experiments of 16 h, and [BQ]/[Pd] = 40 for the experiments of 24 h.

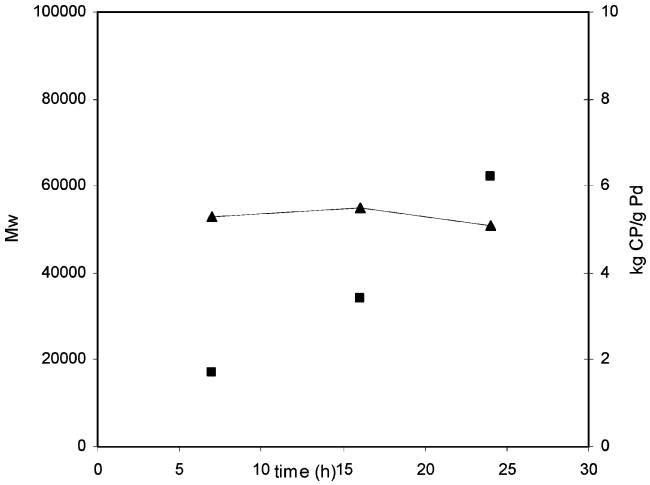

Figure 11. CO/ethylene copolymerization reaction: effect of reaction time both on productivity and on molecular weight. Catalyst precursor: $[Pd(3\text{-}n\text{Bu-phen})_2][PF_6]_2$. Reaction conditions: see Figure 10. (■) kg CP/g Pd; (▲) M_w.

hand, the molecular weight values are among the highest ever reported for this polyketone.

In contrast with the copolymerization reactions run in methanol in the presence of benzoquinone, in the present CO/vinyl arene copolymerization only one of the two possible catalytic cycles[5b] is operative (Scheme 3). In agreement with MALDI-TOF evidence,[9b] the activation of the bischelated catalyst precursor (**na** species) takes place through two different pathways: (i) the reaction with TFE and CO to yield the trifluorocarboalkoxy species **nb′** or (ii) the reaction with traces of water and CO to give the Pd-hydride intermediate **nb**. Insertion of the olefin into either the Pd−H of **nb** or the Pd−C of **nb′** initiates the growth of the polymeric chain (species **nc** or **nc′**), which proceeds by successive alternating migratory insertions of the two monomers into the Pd−alkyl or Pd−acyl bonds. Possible intermediates in this process are **nd** and **ne**. They can be present both in the homogeneous and in the heterogeneous state and can be viewed as polyketone-supported catalysts. The diverse outcomes of the reaction indicate that the N−N ligand is coordinated to the palladium center, even in the heterogeneous species.

The growth of the polymeric chain is terminated when the Pd-alkyl derivative **ne** undergoes β-hydrogen elimination. This delivers the polyketone with an unsaturated end-group and the Pd-hydride **nb**, which can restart a new polymer chain. Since the polymerization proceeds even in the absence of the oxidant, the Pd−H has to be stable enough to allow for the insertion of one olefin molecule to start a new polymeric chain. The formation of species **nb′** is not possible anymore.

The results evidence that the introduction of an alkyl group in a putatively innocent position of the phenanthroline framework exerts two main effects: (i) to increase the stability of the active species; (ii) to favor the growth of polymeric chains of longer length. The body of results available from our present and previous works on this subject allow us to draw some conclusions and to formulate reasonable hypotheses on the mechanism of the polymerization, even in the absence of direct experimental data.

The use of trifluoroethanol as the solvent in this reaction has several positive effects. First, given its acidity, it removes (or retards) the main decomposition pathway, which involves deprotonation of the intermediate Pd-hydride to a nonstable Pd(0) species (Scheme 3). Basically for the same reason, it provides a Pd-solvate complex, which was shown to be the most stable in the range of several different carbinols.[28] Second, the poor nucleophilicity of this solvent makes it unfit for promoting alcoholysis of Pd-acyl intermediates, and precedent kinetic studies have demonstrated that trifluoroethanol is the least reactive one in a range of different alcohols toward preformed Pd-acyl complexes.[28] Thus, this pathway[9b] is completely suppressed and β-hydrogen elimination becomes the unique termination process for the polymerization. This contributes positively to an increase in the M_w of the polymer.

The results reported in this paper indicate that the alkyl substituent in position 3 of phenanthroline plays a role in determining the molecular weight of the polymer and that sterically demanding substituents cause a pronounced increase of M_w values, regardless of the nature of the aromatic olefin. This effect is due to an increase of the ratio between the propagation and termination rates. Analysis of the TON values (calculated on the assumption that all the metal centers are active catalytic sites; Table 5) evidences that, when styrene is the comonomer, they are more or less the same for the three catalysts. Thus, the increase of the number of inserted repetitive units, obtained with the use of 3-R-phen, might be related to a higher insertion rate with respect to that typical of the phen catalyst, while no effect on the termination rate is apparent. On the other hand, modest but significant differences of TON are observed in the case of *p*-Me-styrene, where the figures of 3-R-phens are consistently lower than those observed with phen. This fact indicates that, with this substrate, 3-alkyl-substituted phens exert a positive effect not only on the insertion rate but also on the

(28) Van Leeuwen, P. W. N. M.; Zuideveld, M. A.; Swennenhuis, B. H. G.; Freixa, Z.; Kamer, P. C. J.; Goubitz, K.; Fraanje, J.; Lutz, M.; Spek, A. L. *J. Am. Chem. Soc.* **2003**, *125*, 5523.

Scheme 3. The Proposed Catalytic Cycle

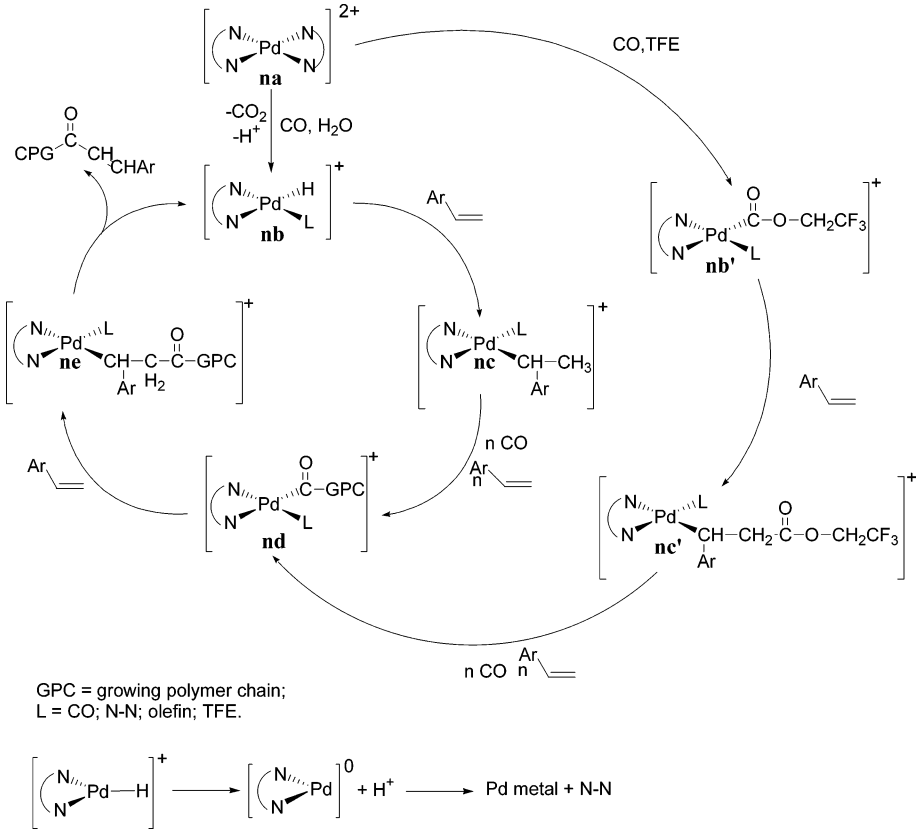

Table 6. Elemental Analyses for Complexes 2a−7a[a]

complex	% C	% H	% N	yield (%)
[Pd(3-Me-phen)$_2$][PF$_6$]$_2$ (**2a**)	39.6 (39.8)	2.51 (2.57)	7.10 (7.14)	78
[Pd(3-Et-phen)$_2$][PF$_6$]$_2$ (**3a**)	41.3 (41.2)	2.92 (2.94)	6.81 (6.89)	74
[Pd(3-*i*Pr-phen)$_2$][PF$_6$]$_2$ (**4a**)	42.7 (42.8)	3.39 (3.36)	6.60 (6.66)	80
[Pd(3-*n*Bu-phen)$_2$][PF$_6$]$_2$ (**5a**)	43.8 (44.2)	3.65 (3.68)	6.48 (6.44)	45
[Pd(3-*s*Bu-phen)$_2$][PF$_6$]$_2$ (**6a**)	44.4 (44.2)	3.70 (3.68)	6.42 (6.44)	84
[Pd(3-tmp-phen)$_2$][PF$_6$]$_2$ (**7a**)	46.6 (46.7)	4.33 (4.37)	6.05 (6.06)	65

[a] Calculated values are reported in parentheses.

termination rate, which is retarded as compared to the unsubstituted phen.

This is most probably a consequence of the inherent disparity of the two N-donors of monosubstituted phens, which can facilitate the dissociation of the least tightly bound N-arm of the bischelated complex to provide the open coordination site necessary for the startup of the catalytic cycle. We may envision that the hemilabile behavior featured by one of the phen units of the bischelated complex may contribute further to the positive outcome of the reaction through the stabilization of any otherwise short-lived intermediate involved in the catalytic cycle.

Finally, the 3-R-phens exert a remarkable positive effect on the copolymerization reaction when vinyl arenes are used, while no effect is observed in the CO/ethylene copolymerization, even when the catalyst containing the most hindered ligand is used.

Conclusions

In this paper we studied the coordination chemistry to Pd(II) of a series of 3-alkyl-substituted-1,10-phenanthrolines. The X-ray analysis of two representatives of the corresponding bischelated complexes, [Pd(3-R-phen)$_2$][PF$_6$]$_2$, shows that, in the solid state, the two molecules of 3-R-phen prefer to bind palladium in a *syn* arrangement, which is indicated to be slightly more stable than the *anti* by density functional theory calculations. Nevertheless, ^{1}H NMR spectroscopy shows the presence, in solution, of an equilibrium between the *syn* and *anti* isomers.

The bischelated dicationic palladium complexes, **2a**−**7a**, are found to be very efficient catalyst precursors for the CO/aromatic olefin copolymerization, in trifluoroethanol, yielding the corresponding syndiotactic polyketones in unprecedentedly high yields and high molecular weight values. These catalytic results appear to be related to the high stability shown by the active species that presents the phenanthroline substituted with a bulky alkyl group in the palladium coordination sphere, in combination with the use of trifluoroethanol as reaction medium.

Experimental Section

General Methods. Commercial [Pd(CH$_3$COO)$_2$] was a loan from Engelhard and used as received. The bidentate nitrogen-donor ligands, 2,2,2-trifluoroethanol, styrene, and *p*-Me-styrene, the reagents for the synthesis of 3-R-phen (Aldrich),

Table 7. Crystal Data and Details of Structure Refinements for Complexes 4a and 5a

	4a	**5a**·(C_3H_6O)
empirical formula	$C_{30}H_{28}F_{12}N_4P_2Pd$	$C_{35}H_{38}F_{12}N_4OP_2Pd$
fw	840.90	927.03
cryst syst	monoclinic	monoclinic
space group	*C*2/*c* (No.15)	*P*2/*c* (No.13)
a (Å)	13.674(2)	8.168(2)
b (Å)	14.796(2)	15.140(2)
c (Å)	16.422(2)	15.606(2)
β (deg)	101.63(1)	95.83(1)
V (Å^3)	3254.3(8)	1919.9(6)
T (K)	293(2)	293(2)
Z	4	2
ρ_{calcd} (g cm^{-3})	1.716	1.604
2θ range (deg)	2.05−29.97	2.51−27.10
μ Mo Kα (mm^{-1})	0.767	0.660
no. of obsd unique reflns	4740	4630
no. of params	246	299
R_1[a]	0.0506	0.0657
wR_2[b]	0.1459	0.1495
GOF on F^2[c]	1.060	0.957
residuals, e Å^{-3}	0.960, −0.616	0.404, −0.714

[a] $R_1 = \sum| |F_o| - |F_c| |/\sum|F_o|$. [b] $wR_2 = [\sum w(F_o^2 - F_c^2)^2/\sum w(F_o^2)^2]^{1/2}$. [c] GOF = $[\sum w(F_o^2 - F_c^2)^2/\sum(n - p)]^{1/2}$.

and analytical grade solvents (Baker) were used without further purification for synthetic, spectroscopic, and catalytic purposes. Carbon monoxide (CP grade, 99.9%) as well as CO/ethylene 1:1 mixture were supplied by SIAD.

The 3-alkyl-substituted-phen were synthesized according to the literature.[19]

IR spectra were recorded on a Perkin-Elmer 983 G spectrometer as Nujol mulls. ^{1}H NMR spectra of the ligands and the complexes were recorded at 400 MHz on a JEOL EX 400 spectrometer operating in Fourier transform mode; ^{13}C NMR spectra were recorded on the spectrometer at 100.5 MHz. Solvents used for NMR spectra include $CDCl_3$ and DMSO-d_6 for the ligands and the palladium complexes, and 1,1,1,3,3,3-hexafluoro-2-propanol (HFIP) with a small amount of $CDCl_3$ for locking purposes for the polyketones. All spectra were referenced to the peak of undeuterated solvents: for ^{1}H NMR spectra, 2.50 ppm for DMSO-d_6, 7.26 ppm for $CDCl_3$, and 5.30 ppm for CD_2Cl_2; and for ^{13}C NMR spectra, 77.0 ppm for $CDCl_3$ in HFIP.

Elemental analyses (C, H, N), performed at Dipartimento di Scienze Chimiche, Università di Trieste (Italy), were in perfect agreement with the proposed stoichiometry (Table 6).

Synthesis of Complexes [Pd(N−N)$_2$][PF$_6$]$_2$. The bischelated derivatives [Pd(N−N)$_2$][PF$_6$]$_2$ (N−N = phen, dmphen, tmphen, 3-R-phen) were synthesized according to the procedures already reported by us.[9a,20]

The Two-Step Procedure. Synthesis of Complexes [Pd(CF$_3$COO)$_2$(3-R-phen)] (3-R-phen = 1−4, 6, 7). A 0.19 mmol sample of the ligand is added, at room temperature, to a methanolic solution of [Pd(CH$_3$COO)$_2$] (0.16 mmol in 5 mL of CH$_3$OH). The solution becomes darker, and after complete dissolution of the ligand, it is filtered over fine paper. An excess of CF$_3$COOH (0.35 mL) with respect to palladium is added, changing the color of the solution from red-brown to yellow. The product precipitates as a yellow solid upon concentration of the solution to half volume. It is removed by filtration, washed with cold methanol, and vacuum-dried.

Synthesis of Complexes [Pd(3-R-phen)$_2$][PF$_6$]$_2$ (1a−4a, 6a, 7a). The proper ligand, 3-R-phen (0.06 mmol), is added, at room temperature, to a methanolic suspension of [Pd(CF$_3$COO)$_2$(3-R-phen)] (0.05 mmol in 2 mL of CH$_3$OH; Pd:3-R-phen = 1:1.2), yielding a yellow-orange solution. To this solution is added NaPF$_6$, dissolved in a minimum amount of methanol (Pd:PF$_6^-$ = 1:2.2), giving the precipitation of the product as a yellow solid. After 15 min under stirring, at room temperature, the solid is removed by filtration, washed with cold methanol, and vacuum-dried.

The One-Pot Procedure. Synthesis of Complex [Pd(3-*n*Bu-phen)$_2$][PF$_6$]$_2$ (5a). [(3-*n*Bu-phen)H][PF$_6$] (0.66 mmol) is added to a filtered solution of [Pd(CH$_3$COO)$_2$] in acetone (0.33 mmol in 5 mL), at room temperature, under stirring, yielding a red solution, from which the product precipitates as a yellow solid after 15 min. After 30 min the solid is removed by filtration, washed with diethyl ether, and vacuum-dried.

X-ray Analysis. Single crystals suitable for X-ray analysis of complexes **4a** and **5a** are obtained with the double-layer method by dissolving 20 mg of the complex in 1.5 mL of acetone. Three milliliters of $CHCl_3$ is slowly stratified under the filtered solution.

Unit cell parameters were obtained by least squares treatment of 25 reflections in the θ range 12−19°. Measurements were carried out at room temperature using $\omega-2\theta$ scan technique on a CAD4 Enraf-Nonius diffractometer, equipped with graphite-monochromator and Mo Kα radiation (λ = 0.71073 Å). Three standard reflections, measured at regular intervals throughout the data collections, showed an intensity decay of 38.3% for the butyl derivative. An absorption correction, based on the empirical ψ-scan method, was applied to both data sets. The structures were solved by conventional Patterson[29] and Fourier methods and refined by full-matrix least squares on F^2 by the SHELX97 package.[29] The alkyl groups of both the complexes were found disordered over two conformations (occupancies refined to 0.64/0.36(3) and 0.66/0.34(2), respectively). In **5a** one of the two PF_6^- anions was found disordered over two orientations (50% occupancy), and the ΔF map revealed a lattice molecule of acetone. All the calculations were performed using the WinGX System, Ver 1.63.[30]

Theoretical Analysis. The electronic structure of the systems considered in this work has been obtained solving the Kohn−Sham (KS) equations, according to the density functional theory (DFT) formalism.[31] The ADF program[32] using a LCAO implementation has been employed to solve the KS equations. The basis sets belonging to the ADF database have been adopted, of the following types: Pd TZP frozen core 3d, N and C DZP frozen core 1s, H DZP. This choice has proven accurate and computationally economic in previous works on transition metal complexes.[33] For the geometry optimizations the local density approximation for the exchange−correlation functional has been employed, with the VWN parametrization,[34] while for a more accurate calculation of the relative energy differences between *syn* and *anti* isomers a single-point calculation with GGA BP functional[35,36] has been applied.

CO/Aromatic Olefin Copolymerization Reactions. The reactions were carried out in a stainless steel autoclave (150 mL), equipped with a Teflon liner, magnetic stirrer, heating mantle, and temperature controller. The complex, the aromatic olefin, and the solvent (TFE) were placed in the reactor, which was then pressurized with CO and heated. After cooling and releasing the residual gas, methanol (200 mL) was added. The copolymer was separated by filtration, washed with methanol, and dried under vacuum.

CO/Ethylene Copolymerization Reactions. The reactions were carried out following the same technique reported for the CO/aromatic olefin copolymerization with two differences: (i) 1,4-benzoquinone was added to the reaction mixture

(29) Sheldrick, G. M. *SHELX97* Programs for Crystal Structure Analysis (Release 97-2); University of Göttingen: Germany, 1998.
(30) Farrugia, L. J. *J. Appl. Crystallogr.* **1999**, *32*, 837.
(31) Parr, R. G.; Yang, W. *Density Functional Theory of Atoms and Molecules*; Oxford University Press: New York, 1989.
(32) Baerends, E. J.; Ellis, D. E.; Roos, P. *Chem. Phys.* **1973**, *2*, 41.
(33) Stener, M.; Calligaris, M. *J. Mol. Struct.* (*THEOCHEM*) **2000**, *497*, 91.
(34) Vosko, S. H.; Wilk, L.; Nusair, M. *Can. J. Phys.* **1980**, *58*, 1200.
(35) Becke, A. D. *Phys. Rev. A* **1988**, *38*, 3098.
(36) Perdew, J. P. *Phys. Rev. B* **1986**, *33*, 8822.

before closing the reactor; (ii) the autoclave was pressurized with a 1:1 mixture of CO/ethylene.

Molecular Weight Measurements of CO/Aromatic Olefin Polyketones. The molecular weights ($\langle M_w \rangle$) of copolymers and the molecular weight distributions ($\langle M_w \rangle / \langle M_n \rangle$) were determined by gel permeation chromatography versus polystyrene standards. The analyses were recorded on a Knauer HPLC (K-501 pump, K-2501 UV-detector) with a PLgel 5 μm 10^4 Å GPC column and chloroform as solvent (flow rate 0.6 mL/min). The CO/styrene copolymer was dissolved as follows: 3 mg of the sample was solubilized with 120 μL of 1,1,1,3,3,3-hexafluoro-2-propanol, and chloroform was added up to 10 mL, while the CO/*p*-Me-styrene copolymer was directly soluble in chloroform. The statistical calculations were performed using the Bruker Chromstar software program.

Molecular Weight Measurements of CO/Ethylene Polyketones. The molecular weight values of the CO/ethylene polyketones were measured at Shell Research and Technology Centre, Amsterdam, by GPC using methyl methacrylate for calibration purposes.

Acknowledgment. This work was supported by Ministero dell'Istruzione, dell'Università e della Ricerca (MIUR−Rome; PRIN No. 2003033857 and PRIN No. 2003039774) and by the European Network "PALLADIUM" (Fifth Framework Program, contract No. HPRN-CT-2002-00196). Engelhard Italiana is gratefully acknowledged for a generous loan of $[Pd(CH_3COO)_2]$. The Shell Research and Technology Centre, Amsterdam, is acknowledged for the measurements of molecular weight of CO/ethylene polyketones.

Supporting Information Available: NMR spectra of complex **4a** recorded after the addition of different amounts of the free ligand **4** and cif files of the crystal structures. This material is available free of charge via the Internet at http://pubs.acs.org.

OM0493412